Polymer Chemistry

ROYAL SOCIETY OF CHEMISTRY

PAPER

View Article Online
View Journal | View Issue

Check for updates

Cite this: *Polym. Chem.*, 2025, **16**, 2751

Synthesis of electron-deficient polymers based on sulfur-bridged dithienylboranes as a building block†

Yohei Adachi, *[a] Ryuji Matsuura,[a] Mitsuru Sakabe,[a] Hiroki Tobita,[a] Hideki Murakami[b] and Joji Ohshita *[a,c]

Received 28th February 2025,
Accepted 12th May 2025

DOI: 10.1039/d5py00203f

rsc.li/polymers

π-Conjugated materials incorporating tricoordinate boron are known to possess relatively deep LUMO energy levels owing to the interaction between the empty p orbital of boron and the π* orbital. However, polymers with simple triarylborane structures do not have deep LUMO energy levels for applications in electron-accepting optoelectronic materials, such as n-type semiconductors. In this study, we synthesized new p–π* conjugated polymers by copolymerizing thiaborin units containing boron and sulfur atoms and diketopyrrolopyrrole (DPP), a well-known acceptor unit. The resulting polymers exhibited extended conjugation through the boron p orbital and strong absorption in the visible to near-infrared region. Although these polymers did not show n-type semiconductor behavior, they possessed deep LUMO energy levels lower than −3.6 eV. Furthermore, titration experiments using an amine base revealed that the polymer containing a sulfone unit has strong Lewis acidity, as evidenced by changes in the UV-vis absorption spectrum upon coordination of the base.

Introduction

π-Conjugated polymers are widely utilized in various applications, including organic electronic devices,[1–3] and numerous conjugated polymers with diverse building blocks have been synthesized. Among the building blocks of π-conjugated polymers, electron-deficient units, such as benzothiadiazole (BT) and diketopyrrolopyrrole (DPP), are indispensable for the development of donor–acceptor (D–A) type polymers[4,5] and n-type semiconducting polymers.[6–8] Consequently, the synthesis of new electron-deficient units has been actively pursued. On the other hand, tricoordinate boron, which possesses an empty 2p orbital, generally exhibits electron-accepting characteristics.[9–12] D–A type polymers employing tricoordinate boron as an acceptor have been extensively reported.[13–20] For example, Jäkle and co-workers synthesized dithienylborane (**^{F}BDT**, Fig. 1) with a bulky tris(2,4,6-trifluoromethylphenyl) (^{F}Mes) group and reported p–π* conjugated polymers that used ^{F}BDT as a building block.[13] Helten and co-workers developed polymers by combining furan and tricoordinate boron.[15,16] However, the electron-accepting ability of tricoordinate boron is inferior to that of typical π-conjugated acceptor units, such as BT and DPP (Fig. S1†). For example, we showed in our previous study that a D–A type polymer composed of ^{F}BDT and dithienosilole, a strong electron-donating unit, exhibited a relatively wide bandgap of 2.07 eV and weak dependence of its fluorescence spectra on solvent polarity.[14] Furthermore, the two thiophene rings in the BDT framework demonstrated reduced coplanarity owing to steric repulsion caused by the internal β-hydrogens, potentially diminishing intermolecular interactions in the solid state. Although several

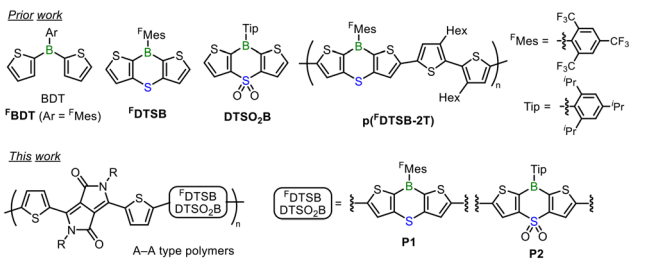

Fig. 1 Dithienylborane-based building blocks and their polymers.

[a]*Smart Innovation Program, Graduate School of Advanced Science and Engineering, Hiroshima University, Higashi-Hiroshima 739-8527, Japan. E-mail: yadachi@hiroshima-u.ac.jp, jo@hiroshima-u.ac.jp*
[b]*Kurume College, National Institute of Technology, Kurume, Fukuoka 830-8555, Japan*
[c]*Division of Materials Model-Based Research, Digital Monozukuri (Manufacturing) Education and Research Center, Hiroshima University, Higashi-Hiroshima, Hiroshima 739-0046, Japan*

†Electronic supplementary information (ESI) available: Experimental details with synthesis, characterization; absorption spectra; DFT computation results; NMR/mass spectra. See DOI: https://doi.org/10.1039/d5py00203f

n-type semiconductor materials based on p–π* conjugated systems have been reported, the drawbacks of the triarylborane units leave significant room for performance improvement.[21] Inspired by the development of a new dithienylborane building block,[22] we have previously synthesized **^{F}DTSB** (Fig. 1), a sulfur-bridged dithienylborane with a ^{F}Mes group on boron, and its polymer **p(^{F}DTSB-2T)** (Fig. 1).[19] This polymer exhibited significantly red-shifted absorption in the solid state compared to in solution, indicating that the introduction of sulfur and the improved coplanarity of the thiophene rings enhanced intermolecular interactions in the p–π* conjugated polymer. Additionally, we reported that **DTSO$_2$B** (Fig. 1), obtained by oxidizing the sulfur atoms in the **DTSB** structure, showed a lowered LUMO energy level caused by the sulfur oxidation (Fig. S1†), making it a strong electron-acceptor unit.[23] In this study, we synthesized new electron-deficient acceptor–acceptor (A–A) type p–π* conjugated polymers containing sulfur-bridged dithienylborane units (**^{F}DTSB** and **DTSO$_2$B**) copolymerized with DPP (Fig. 1). Electrochemical measurements revealed that these polymers possessed deep LUMO energy levels, demonstrating that the **^{F}DTSB** and **DTSO$_2$B** units worked effectively as acceptor units in electron-deficient polymers.

Results and discussion

Synthesis

The synthetic route of the p–π* conjugated polymers is shown in Scheme 1. To enhance polymer solubility, a 2-hexyldecyl group was introduced onto the nitrogen atoms of the DPP unit. The **DTSB** and **DTSO$_2$B** units had different aryl groups on the boron atom because the ^{F}Mes group could not be introduced to the **DTSO$_2$B** monomer.[23] The A–A type p–π* conjugated polymers were synthesized *via* a palladium-catalyzed Stille cross-coupling reaction between the distannylated **DTSB** or **DTSO$_2$B** monomer and the dibrominated DPP comonomer. It should be noted that **^{F}DTSB-Sn** contains tributylstannyl groups, while **DTSO$_2$B-Sn** contains trimethylstannyl groups. This is because the synthesis of these stannylated monomers has already been established.[19,23] First, we synthesized copolymer **P1-EH** from **DPP-Br2** bearing 2-ethylhexyl groups on the nitrogen atoms and **^{F}DTSB-Sn**. However, **P1-EH** was poorly soluble, and the yield after the purification by Soxhlet extraction using chloroform was only 15%. To improve polymer solubility, the alkyl groups on the nitrogen atoms were replaced with 2-hexyldecyl groups, and polymers **P1-HD** and **P2-HD** were synthesized using the DPP monomer with 2-hexyldecyl groups. The crude polymers with the 2-hexyldecyl groups were purified by removing the palladium catalyst with a short silica pad, followed by reprecipitation from ethanol/chloroform. **P1-HD** and **P2-HD** were soluble in organic solvents, such as chloroform and THF, and their yields were good (Scheme 1). GPC analysis using polystyrene standards revealed number-average molecular weights (M_n) of 18 000, 20 000, and 10 900 for **P1-EH**, **P1-HD**, and **P2-HD**, respectively, confirming the formation of sufficiently high molecular weight polymers. In the case of **P1-EH** and **P1-HD**, significant signal broadening was observed in the ^{1}H NMR spectra, and signals corresponding to the thiophene rings and the ^{F}Mes group were detected in the aromatic region (Fig. S2†). In the case of **P2-HD**, the ^{1}H NMR spectrum was well resolved, and all peaks could be clearly assigned (Fig. S2†), which may be due to the lower molecular weight and higher solubility of **P2-HD** in $CDCl_3$ compared to **P1**. In the ^{11}B NMR spectrum of **P2-HD**, a broad peak was observed at 45 ppm (Fig. S3†), indicating that the boron center in the polymer is tricoordinate. In the ^{11}B NMR spectra of **P1-EH** and **P1-HD**, a broad peak was observed at approximately 33 ppm (Fig. S3†), which appeared at a higher field than those of **P2-HD** and typical p–π* conjugated polymers.[13,15,16] Although the reason for this is unclear, a similar observation has been reported in p–π* conjugated polymers based on the **^{F}DTSB** unit.[19] The ^{19}F NMR spectrum of **P1-HD** displayed two signals attributable to the ^{F}Mes group (Fig. S4†), suggesting that the **^{F}DTSB** unit is preserved within the polymer structure. To further analyze the polymer structures, MALDI-TOF mass spectrometry was conducted (Fig. S5†). For **P1-EH**, most of the observed peaks could be assigned to the expected polymer structure, suggesting that structural defects were minimal. In contrast, the mass spectrum of **P1-HD** showed signals corresponding to the repeating units, similar to **P1-EH**, but also displayed additional peaks indicative of structural defects. Notably, molecular ion peaks corresponding to species containing greater numbers of DPP units than **^{F}DTSB** units were observed, implying that homocoupling of DPP units occurred during the polymerization of **P1-HD** (Fig. S5†). Since homocoupling reactions are known to be promoted at high temperatures,[24] it may be possible that in the case of the poorly soluble **P1-EH**, the polymer was precipitated from the reaction medium at an early stage, thereby suppressing further homocoupling. In the mass spectrum of **P1-HD**, butyl-terminated structures were also detected (Fig. S5†), which are likely formed through the transmetalation of butyl groups from tributyltin groups during the cross-coupling reaction. For **P2-HD**, although the precise structure of the end groups could not be verified from the mass spectrum, repeating units corresponding to DPP and **DTSO$_2$B** units were observed (Fig. S5†), indicating the presence of an ideal structure in the polymer. Thermogravimetric (TG) analysis in air revealed that the 5% weight loss temperature (T_d^5) of **P1-HD** was 354 °C while that of **P2-HD** was 280 °C, indicating that **P1-HD** possesses higher thermal stability than **P2-HD** (Fig. S6†). This difference could be attributed to the difference of the aryl substituent on the

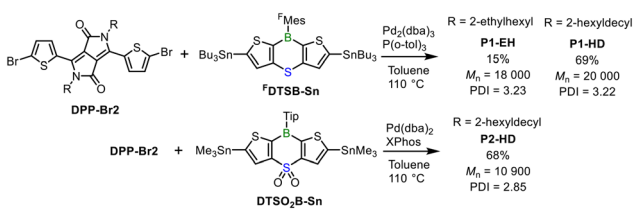

Scheme 1 Synthetic scheme of **DTSB/DTSO$_2$B**-containing polymers.

boron atom.[14] The T_d[5] of **p(FDTSB-2T)**, which has an **FDTSB** unit like **P1-HD**, was 328 °C,[19] demonstrating that copolymerization with the DPP unit slightly enhances the thermal stability of the p–π* conjugated polymer.

Optical properties

Next, the UV-vis absorption spectra of the p–π* polymers were measured in toluene (Fig. 2). The maximum absorption wavelengths of **P1-EH**, **P1-HD**, and **P2-HD** were observed at 722, 721, and 719 nm, respectively (Table 1), representing a redshift of over 280 nm compared to **p(FDTSB-2T)** (λ_{max} = 433 nm in toluene).[19] This redshift is attributed to the effective conjugation of the DPP unit. The maximum absorption wavelength of **p(FBDT-DPP)**, a DPP-based p–π* conjugated polymer without sulfur bridging (Fig. 2a), was observed at 594 nm in chlorobenzene.[21] This demonstrates that sulfur bridging improves the coplanarity of the thiophene rings and reduces the HOMO–LUMO energy gap. On the other hand, the maximum absorption wavelength of **p(4T-DPP)**, a fully conjugated polymer composed of DPP and quaterthiophene (Fig. 2a), was 777 nm in chloroform,[25] indicating that the conjugation through thiaborin rings causes a slight widening of the band gap. Although **P1-EH** and **P1-HD** share the same structure in the main chain, differing only in the alkyl group on the nitrogen atoms, their spectra markedly differed (Fig. 2b). The absorption spectrum of **P1-EH** exhibited apparent vibrational features for the 0–0 and 0–1 transitions, suggesting a rigid main-chain structure. On the other hand, the absorption spectrum of **P1-HD** showed a maximum at a similar wavelength and significantly broadened shoulder peaks in the longer wavelength region. The appearance of the shoulder peaks can be attributed to two possible reasons. One is the structural defects, including the homocoupled DPP units, as suggested by the MALDI-TOF mass spectrum (Fig. S5†). The other reason is the potential aggregation of the polymer even in solution.[26] The absorption bands of **P2-HD** appeared in a similar region to those of **P1-EH**, suggesting that the oxidation of sulfur does not significantly affect the HOMO–LUMO energy gap in these polymers. The optical band gaps (E_g^{opt}) of the polymers were determined from the absorption edges (Table 1). In toluene, the E_g^{opt} values for **P1-EH**, **P1-HD**, and **P2-HD** were 1.46, 1.31, and 1.48 eV, respectively, significantly smaller than that of **p(FBDT-DPP)** (1.83 eV).[21] Notably, the E_g^{opt} of **P2-HD** was comparable to that of fully conjugated polymer **p(4T-DPP)** (1.2 eV).[25] To investigate the influence of solvent polarity, the UV-vis absorption spectra of these p–π* conjugated polymers were measured in THF and dichloromethane in addition to in toluene (Fig. S7†). The absorption spectra of **P1-EH** and **P1-HD** demonstrated negligible changes across different solvents, indicating minimal dependence on solvent polarity in the ground state. On the other hand, the absorption spectra of **P2-HD** exhibited a slight blue shift in dichloromethane and THF compared to that in toluene. This shift may be attributed to aggregation, possibly because of the low solubility of **P2-HD** in toluene (*vide infra*).

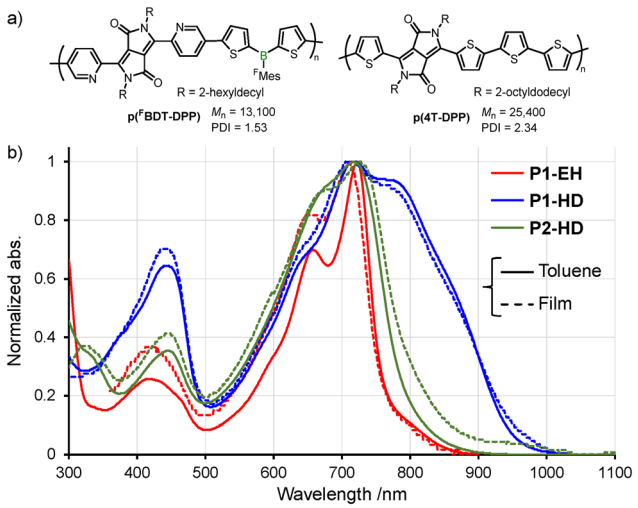

Fig. 2 Chemical structures of previously reported DPP polymers (a) and UV-vis absorption spectra of **DTSB/DTSO$_2$B**-containing polymers in toluene and as film (b).

Next, the UV-vis absorption spectra of the spin-coated thin films were measured (Fig. 2b). The absorption spectrum of **P1-EH** in the film was nearly identical to that in solution. In contrast, the absorption spectrum of **P2-HD** in the film showed a slight redshift compared to that in solution, suggesting the presence of π–π interactions in the solid state. The absorption spectrum of **P1-HD**, similar to that of **P1-EH**, exhibited minimal differences between the film and the solution; however, the prominent shoulder peaks may suggest aggregation even in solution for **P1-HD**. To investigate this, temperature-dependent UV-vis absorption spectra were measured in toluene (Fig. S8†). For **P1-EH**, only a slight decrease in the absorption band corresponding to the 0–0 transition was

Table 1 Optical and electrochemical properties of **DTSB/DTSO$_2$B**-containing polymers

Polymer	λ^{abs} (film)[a]/nm	E_g^{opt} (film)[b]/eV	V_{red}[c]/V	V_{ox}[d]/V	LUMO[e]/eV	HOMO[f]/eV	E_g^{CV}[g]/eV
P1-EH	722 (712)	1.46 (1.46)	−1.23	0.50	−3.57	−5.30	1.73
P1-HD	721 (714)	1.31 (1.29)	−1.23	0.54	−3.57	−5.34	1.77
P2-HD	719 (728)	1.48 (1.41)	−1.19	0.72	−3.61	−5.52	1.91

[a] Absorption maximum in toluene and in film. [b] Band gap estimated from the absorption edge in toluene and in film. [c] Onset potential of the reduction wave of film. [d] Onset potential of the oxidation wave of film. [e] LUMO = −4.8 − V_{red}. [f] HOMO = −4.8 − V_{ox}. [g] Band gap estimated from V_{ox} and V_{red}.

observed with increasing temperature. On the other hand, **P1-HD** exhibited an obvious decrease in the shoulder peaks with increasing temperature, suggesting that these shoulder peaks partially originate from aggregation.[26] To further examine the aggregation behavior, UV-vis absorption spectra of **P1-HD** were measured at various concentrations. However, the intensity of the shoulder peaks remained unchanged even at low concentrations, indicating the no concentration dependence (Fig. S9†). These results suggest that **P1-HD** may form aggregates even at low concentrations, or that the shoulder peaks are largely attributable not only to aggregate but also to the structural defects arising from the homocoupled DPP units. The impact of the structural defects on the UV-vis absorption spectra is discussed in detail in the section on DFT calculations. **P2-HD** showed a blue shift in its absorption band with increasing temperature (Fig. S8c†), suggesting partial aggregation in toluene at room temperature. The shoulder peaks in the absorption spectrum of **P1-HD** and the redshifted absorption of **P2-HD** in the film relative to that in solution may indicate the presence of strong intermolecular interactions in the solid state, which are usually not observed in p–π* conjugated polymers, including **p(FBDT-DPP)**.[21] These results suggest that sulfur-atom bridging can enhance intermolecular interactions in p–π* conjugated polymers.

DFT calculations

To analyze the electronic structures of the polymers, DFT calculations were performed on oligomers with a degree of polymerization n of 2.5, namely, **O1-Me** and **O2-Me**, as models for the respective polymers (Fig. 3). For comparison of structures, similar calculations were also conducted on a model of **p(4T-DPP)**, **o(4T-DPP)**, and a p–π* conjugated oligomer without sulfur bridges, **o(FBDT-DPP)**. Fig. 3 shows the optimized structures and the frontier orbitals of these oligomers. In **o(4T-DPP)**, all the π-conjugated units were perfectly coplanar. Similarly, the main chains of thiaborin-based p–π* conjugated oligomers, **O1-Me** and **O2-Me**, were nearly coplanar. In contrast, **o(FBDT-DPP)**, lacking the sulfur bridges, exhibited significant twisting between the two thiophene rings within the FBDT unit, with a dihedral angle of 36.5°. This is caused by the steric hindrance from β-hydrogen atoms on the thiophene rings. The HOMO is delocalized across the entire **o(4T-DPP)** molecule, while in p–π* conjugated oligomers, it is localized on the DPP unit owing to the interruption of conjugation at the boron bridge. Consequently, the HOMO energy levels of p–π* conjugated systems are much deeper than that of **o(4T-DPP)** (Fig. 3). The LUMO in all molecules is delocalized across the central DPP and peripheral oligothiophene units, with a clear contribution from the p orbital of boron in p–π* conjugated oligomers. Similar to the HOMO energy levels, the LUMO energy levels of the p–π* conjugated oligomers are also much deeper than that of **o(4T-DPP)** (Fig. 3). Notably, the LUMO energy level of the sulfone-containing **O2-Me** is the lowest among these oligomers, at −3.36 eV.

To further investigate the impact of the structural defects observed in **P1-HD**, a geometry optimization was performed

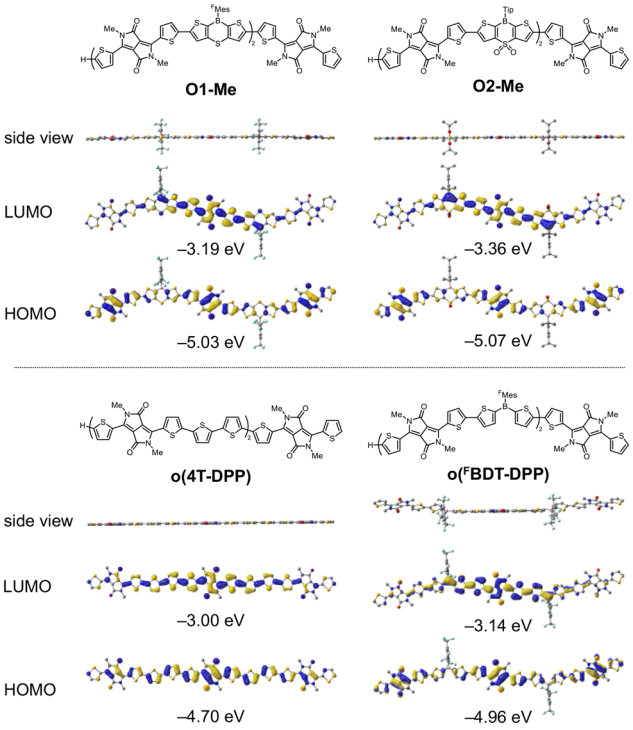

Fig. 3 DFT-optimized structures and frontier orbitals of DPP-containing model oligomers at the B3LYP-D3BJ/6-31G(d) level.

for an oligomer model **O1-Me′**, in which the connectivity of one **FDTSB**-DPP unit in **O1-Me** was reversed. Subsequent TD-DFT calculations were performed to evaluate the $S_0 \rightarrow S_1$ electronic transitions (Tables S1 and S2†). Despite no significant difference in planarity between **O1-Me** and **O1-Me′**, the calculated $S_0 \rightarrow S_1$ transition wavelength was 759 nm for **O1-Me** and 838 nm for **O1-Me′** (Fig. S10†), indicating a substantial redshift in absorption induced by the presence of the DPP homocoupling unit. This result supports that the shoulder peaks observed in the UV-vis absorption spectra of **P1-HD** are significantly contributed from the structural defects.

Cyclic voltammetry and evaluation of carrier-transport properties

To investigate the redox properties of the p–π* conjugated polymers, cyclic voltammetry (CV) measurements were conducted on the polymer films (Fig. 4). The frontier orbital energy levels were calculated from the onset potentials of the first oxidation and reduction waves. The LUMO energy levels of **P1-HD** and **P2-HD** were determined to be −3.57 eV and −3.61 eV, respectively (Table 1), indicating deep LUMO energy levels. In particular, **P2-HD** exhibited a slightly deeper LUMO energy level than **P1-HD**, consistent with the results of DFT calculations. This indicates that the sulfone structure effectively contributes to lowering the LUMO energy level. The LUMO energy level of the non-sulfur-bridged polymer **p(FBDT-DPP)** was reported to be −3.58 eV,[21] and the thiaborin-based polymers exhibited comparable or even deeper LUMO energy levels. These obser-

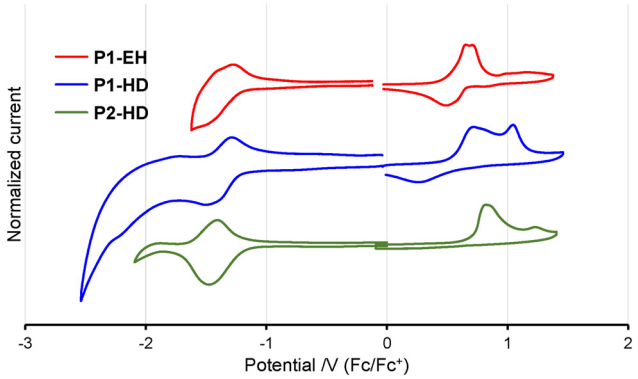

Fig. 4 Cyclic voltammograms of **DTSB/DTSO$_2$B**-containing polymer films in acetonitrile with 0.1 M TBAPF$_6$ at a scan rate of 100 mV s^{-1}.

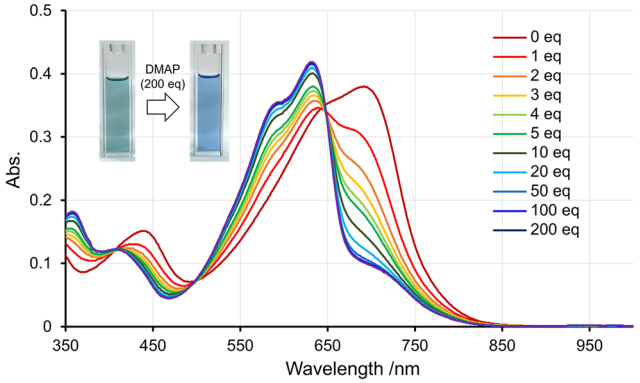

Fig. 5 UV-vis absorption data obtained from titrations of **P2-HD** with DMAP aliquots in $CHCl_3$ at the concentration of 0.01 mg mL^{-1}. Insets show the response of **P1-HD** and **P2-HD** to the addition of DMAP.

vations confirm that introducing thiaborin structures is an effective strategy for lowering the LUMO energy level in p–π* conjugated materials. Motivated by the extended conjugation and the deep LUMO energy levels of these p–π* conjugated polymers, we fabricated organic field-effect transistors (OFETs) using these polymers to investigate their p- and n-type semiconducting properties. Although these polymers showed good film-forming properties, attempts to evaluate the transistor characteristics of spin-coated films did not yield clear evidence of semiconducting behavior (Fig. S11†). The UV-vis absorption spectra suggested strong intermolecular interactions in these p–π* conjugated polymers (*vide supra*), which are generally advantageous for carrier transport. Nonetheless, one possible reason for the absence of semiconducting properties is that the bulky aryl groups attached to boron increased the intermolecular distance in the film, hindering carrier transport.

Optical responses to Lewis bases

Because p–π* conjugated polymers contain Lewis acidic tricoordinate boron, we investigated their response to Lewis bases. Our previous study has demonstrated that the **DTSO$_2$B** unit, despite having a bulky Tip group on the boron atom, can still form a coordination bond with organic bases, such as 4-dimethylanimopyridine (DMAP).[23] As the amount of DMAP added to a solution of **P2-HD** increased, the long-wavelength absorption band gradually decreased, and a new absorption band appeared around 630 nm (Fig. 5). This is believed to result from the disappearance of the p–π* conjugation upon the coordination of DMAP with boron. In contrast, no change was observed in the absorption spectrum of **P1-HD** upon adding DMAP (Fig. S12†), suggesting no coordination with boron. The difference in response to DMAP is thought to be due to the increased Lewis acidity of boron in the **DTSO$_2$B** unit[23] due to the strong electron-withdrawing properties of sulfone.

Finally, to elucidate the influence of aryl substituents on the boron atom, fluoride ion affinity (FIA) calculations were performed (Fig. S13†).[27] Our previous study has shown that oxidation of sulfur significantly enhances the Lewis acidity of the boron atom, and the FIA value of the sulfone compound **DTSO$_2$B** bearing a Tip group on boron is more than 50 kJ mol^{-1} higher than that of its sulfide counterpart, **DTSB**.[23] When the Tip group was replaced with an ^{F}Mes group, the calculated FIA values of **^{F}DTSB** and **^{F}DTSO$_2$B** were found to be even higher than those of their corresponding Tip analogs. Despite the increased steric bulkiness of the ^{F}Mes group, this increase of the Lewis acidity is attributed to the strong electron-withdrawing properties of the CF_3 groups on the ^{F}Mes group. Moreover, regardless of the aryl substituent, sulfone derivatives consistently exhibited higher FIA values than their corresponding sulfide analogs. Consequently, although **O1-Me** and **O2-Me** possess ^{F}Mes and Tip groups on the boron atoms, respectively, **O2-Me** exhibited a higher FIA value than **O1-Me**. This result is consistent with experimental observations showing that only **P2-HD** formed a complex with DMAP.

Conclusions

We synthesized new electron-deficient polymers by copolymerizing thiaborin-based p–π* conjugated building blocks with a DPP unit. These polymers exhibited an extended π-conjugation through the boron p orbital and possessed a small bandgap. Cyclic voltammetry measurements revealed that the polymers had deeper LUMO energy levels than previously reported p–π* conjugated polymers, demonstrating that the combination of thiaborin and DPP units effectively enhanced the electron-deficient character of the polymer. Unfortunately, these polymers did not exhibit the expected n-type semiconductor characteristics. However, their deep LUMO energy levels suggested that incorporating alternative molecular designs to enhance intermolecular interactions within these polymer backbones could lead to the development of n-type semiconductor materials. Furthermore, titration experiments with DMAP revealed that **P2-HD** retained high Lewis acidity even in the polymer. This finding demonstrates that p–π* conjugated polymers incorporating the **DTSO$_2$B** unit can be utilized as sensor materials for detecting Lewis bases.

Author contributions

Yohei Adachi: conceptualization; funding acquisition; project administration; supervision; writing – original draft; writing – review & editing. Ryuji Matsuura: investigation; visualization. Joji Ohshita: supervision; writing – review & editing.

Data availability

The data supporting this article have been included as part of the ESI.†

Conflicts of interest

There are no conflicts to declare.

Acknowledgements

This work was supported by JSPS KAKENHI Grant Numbers JP22K14666 and JP23K23400.

References

1 Y. Li, *Acc. Chem. Res.*, 2012, **45**, 723.
2 A. Facchetti, *Chem. Mater.*, 2011, **23**, 733.
3 X. Guo, M. Baumgarten and K. Müllen, *Prog. Polym. Sci.*, 2013, **38**, 1832.
4 H. Zhou, L. Yang and W. You, *Macromolecules*, 2012, **45**, 607.
5 C. Liu, K. Wang, X. Gong and A. J. Heeger, *Chem. Soc. Rev.*, 2016, **45**, 4825.
6 H. Sun, X. Guo and A. Facchetti, *Chem*, 2020, **6**, 1310.
7 Y. Lu, J.-Y. Wang and J. Pei, *Chem. Mater.*, 2019, **31**, 6412.
8 S. Griggs, A. Marks, H. Bristow and I. McCulloch, *J. Mater. Chem. C*, 2021, **9**, 8099.
9 L. Ji, S. Griesbeck and T. B. Marder, *Chem. Sci.*, 2017, **8**, 846.
10 X. Yin, J. Liu and F. Jäkle, *Chem. – Eur. J.*, 2021, **27**, 2973.
11 K. Tanaka and Y. Chujo, *Macromol. Rapid Commun.*, 2012, **33**, 1235.
12 H. Helten, *Chem. – Asian J.*, 2019, **14**, 919.
13 X. Yin, F. Guo, R. A. Lalancette and F. Jäkle, *Macromolecules*, 2016, **49**, 537.
14 Y. Adachi, Y. Ooyama, Y. Ren, X. Yin, F. Jäkle and J. Ohshita, *Polym. Chem.*, 2018, **9**, 291.
15 A. Lik, S. Jenthra, L. Fritze, L. Müller, K.-N. Truong and H. Helten, *Chem. – Eur. J.*, 2018, **24**, 11961.
16 L. Fritze, M. Fest, A. Helbig, T. Bischof, I. Krummenacher, H. Braunschweig, M. Finze and H. Helten, *Macromolecules*, 2021, **54**, 7653.
17 C. Xue, M. Peng, Z. Zhang, X. Han, Q. Wang, C. Li, H. Liu, T. Li, N. Yu and Y. Ren, *Macromolecules*, 2022, **55**, 3850.
18 X. Han, C. Xue, Z. Zhao, M. Peng, Q. Wang, H. Liu, N. Yu, C. Pu and Y. Ren, *ACS Macro Lett.*, 2023, **12**, 961.
19 Y. Adachi, M. Sakabe, T. Nomura and J. Ohshita, *Polym. J.*, 2023, **55**, 489.
20 A. F. Alahmadi, X. Yin, R. A. Lalancette and F. Jäkle, *Chem. – Eur. J.*, 2023, **29**, e202203619.
21 B. Meng, Y. Ren, J. Liu, F. Jäkle and L. Wang, *Angew. Chem., Int. Ed.*, 2018, **57**, 2183.
22 Y. Yan, Z. Sun, C. Li, J. Zhang, L. Lv, X. Liu and X. Liu, *Asian J. Org. Chem.*, 2017, **6**, 496.
23 Y. Adachi, R. Matsuura and J. Ohshita, *Organometallics*, 2024, **43**, 829.
24 B. Ma, Q. Shi, X. Ma, Y. Li, H. Chen, K. Wen, R. Zhao, F. Zhang, Y. Lin, Z. Wang and H. Huang, *Angew. Chem., Int. Ed.*, 2022, **61**, e202115969.
25 Y. Li, P. Sonar, S. P. Singh, M. S. Soh, M. van Meurs and J. Tan, *J. Am. Chem. Soc.*, 2011, **133**, 2198.
26 R. Heuvel, F. J. M. Colberts, J. Li, M. M. Wienk and R. A. J. Janssen, *J. Mater. Chem. A*, 2018, **6**, 20904.
27 P. Erdmann, J. Leitner, J. Schwarz and L. Greb, *ChemPhysChem*, 2020, **21**, 987.

